Journal of Applied Spectroscopy, Vol. 77, No. 2, 2010

MULTI-OBJECT SPECTROMETER WITH MICROMIRROR ARRAY

E. S. Voropai,[a*] I. M. Gulis,[a] A. G. Kupreev,[a]
K. N. Kaplevskii,[a] A. G. Kostyukevich,[a] A. E. Radko,[b]
and K. A. Shevchenko[b]

UDC 681.785.554

We have designed and built a multi-object spectrometer with micromirror array as a reconfigurable entrance aperture. In interactive mode, the instrument makes it possible to record both the hyperspectrum of the studied region as a whole and also sets of spectra of arbitrarily specified fragments. In this case, a spectral resolution of 0.8 nm or better is provided in the subranges 400–670 nm and 650–900 nm, aperture ratio of the spectroscopic channel at least 1:5. The analytical characteristics of the instrument make it possible to use it to solve a broad range of problems in modern multi-object spectroscopy and hyperspectroscopy.

Key words: *multi-object spectrometer, hyperspectrometer, micromirror array.*

Introduction. In recent decades, in applied spectroscopy the objects of investigation increasingly often are extended regions of space: fragments of the Earth's surface, a stellar cloud, human tissue, etc. Methods allowing us to obtain the optical spectrum for a large number of small fragments of the studied region with a certain spatial and spectral resolution have acquired the name "multi-object" methods (if the full spatial and spectral image $I(x, y, \lambda)$ is recorded, "hyperspectral" methods). Multi-object spectroscopy and hyperspectroscopy are used in medical diagnostics, for remote (aerospace-based) monitoring of the Earth's surface, in forensics, spectroscopy of single quantum objects, and in astronomy studies [1–5].

Today, hyperspectral images (HSI) are most often obtained by scanning the entrance slit of a dispersive spectrometer over the analyte image (or scanning the image over the slit) or by recording the image through sequentially switched narrow-band spectral filters. The major disadvantages of the first approach are the connection between the spatial resolution and the spectral resolution (both are determined by the slit width), use of mechanical scanning systems, and the relatively long time period required for acquisition of hyperspectral images with sufficient spectral and spatial resolution [6–12]. In the second approach, when using a set of mechanically switched filters, the spectral resolution is usually low, and the use of tunable filters (optoacoustic, electro-optic, interference polarization) does not provide fast response and lets us work only with small aperture angles [13].

Development is underway for alternative approaches potentially promising gains in aperture and HSI acquisition time as a result of a multiplex approach and based on the principles of Fourier transform spectroscopy [14, 15]. However, at this time the instrumentation cannot compete with traditional types of hyperspectrometers.

The use of modern spatial light modulators (SLMs), permitting real-time control of the configuration of the entrance aperture of the imaging spectrometer, is promising for development of new types of hyperspectrometers [16]. The indicated approach has advantages such as the possibility of fast readjustment for operation in different modes, simple realization of the mode with electronically controllable scanning of the entrance slit formed by the SLM, fast recording speed (frame spectrum in milliseconds), software control of the resolution over a broad range, the possibility of substantially speeding up acquisition of hyperspectral data as a result of interactive operation with the option for scanning only the sections of the object that are significant from an information standpoint.

In this paper, we describe our dispersion multi-object spectrometer for the visible spectral range with reconfigurable entrance aperture, built on the basis of a spatial light modulator: a micromirror array. The instrument was in-

*To whom correspondence should be addressed.

[a]Belorussian State University, 4 prosp. Nezavisimosti, Minsk 220030; e-mail: voropay@bsu.by; [b]A. N. Sevchenko Scientific Research Institute for Applied Physical Problems, Minsk, Belarus. Translated from Zhurnal Prikladnoi Spektroskopii, Vol. 77, No. 2, pp. 305–312, March–April, 2010. Original article submitted October 9, 2009.

itially aimed at application for scientific research in the field of photodynamic therapy (determination of the location and also the time variation in the distribution of the photosensitive dye in the tissues), but because of its functional flexibility can be used to solve many other problems in modern hyperspectroscopy.

Principles of Operation and Features of the Optical System. The basic principle for acquisition of hyperspectral images in a studied region of space is scanning it with an entrance slit formed using a spatial light modulator (SLM), standing at the entrance to a dispersive imaging polychromator. At the exit from the polychromator is a photodetector array sequentially recording the spectral distributions of quasi-one-dimensional sources: fragments of the object isolated by the slit.

Our analysis has shown that it is expedient to use micromirror devices (arrays) called DMDs (Digital Micromirror Devices), commercially produced by Texas Instruments for use in projectors, as the SLM rather than the currently most widely used liquid-crystal spatial light modulators. Such an array is an ordered two-dimensional structure containing ~10^6 micromirrors of size 10–15 μm each, which can be independently switched between two states described by the tilt of the plane of the element by a ±10–12° angle relative to the normal to the plane of the array. Modern DMDs provide high spatial resolution (~10^6 pixels) and high temporal resolution (switching speed ~30 μsec), high contrast, low light losses, high fill factor (>90%), almost complete lack of spectral and polarization selectivity, and high reliability.

Ref. [16] describes application of a DMD as a reconfigurable entrance aperture for the RITMOS multi-object spectrometer, a unique instrument with complex aspherical refractive and reflective optics, designed for astronomy applications demanding high resolution with a small working spectral range. The DMD replaces a mask with holes isolating images of stellar objects on the entrance aperture of a dispersive spectrometer.

Our hyperspectrometer can operate both in interactive multi-object mode and in spectral hypercube recording mode. In the first mode, an additional observation channel is operative, making it possible to select fragments of interest in the studied region of the object, after which their spectra are simultaneously recorded. This makes possible on-the-fly comparison of the spectra and observation of their time variation. In the second mode, the fragment of the entrance field is scanned by the slit formed from the DMD pixels, and then the matrix of the intensity dependence on three coordinates is constructed: $I(x, y, \lambda)$.

As the spatial light modulator, we chose a Texas Instruments micromirror array (DMD), 0.55″ diagonal XGA with resolution 1024 × 768, size of active region 11.0 × 8.3 mm, micromirrors 10.8 × 10.8 μm. A personal computer was used for general control of the DMD (specification of the configuration of the aperture, slit width, scanning parameters); the DMD control system was interfaced with the computer by means of our own controller board.

Owing to a characteristic feature of the DMD (each micromirror during operation can be found in one of two states, with tilt angle relative to the plane of the array of +12° or −12°), we designed two individual optical channels: a spectroscopic channel and an observation channel. Light beams from fragments of the region of space imaged using the projection system on the DMD are guided into the observation channel for observation and specification of the aperture configuration, or into the spectral channel for spectral imaging.

In designing the optical system of the multi-object spectrometer (Fig. 1), we bore in mind a number of requirements for the aberration and optical aspects and also the technical and technological aspects. The most critical part of the system is the polychromator of the spectral channel, since it should be an imaging polychromator and operate with an extended section of the entrance field. Each of the possible variants for the system was tested using the size and configuration of scattering spots in the image plane in the spectral channel as the test criterion. The optical system of the hyperspectrometer calls for the use of mirror optics (mirror objectives, reflective diffraction grating) in the polychromator of the spectral channel, accordingly ensuring achromaticity of the optical system in the working range.

The optical calculations and modeling showed that in the polychromator, it is reasonable to use spherical optics as the collimator and camera objectives. Parabolic mirrors do not work as well with extended radiation sources [17] and even for small defocusing, considerably degrade the quality of the image on the detector.

Systems with concave diffraction gratings are characterized by either high depth of astigmatic focus over the image field (Rowland, Eagle mounts), which complicates operation with the detector array, or curvature of the image field (Woodsworth mount), which makes implementation of the polychromator difficult [18], so as the dispersive element we chose a flat diffraction grating. The major factors affecting the image quality in the polychromator of the

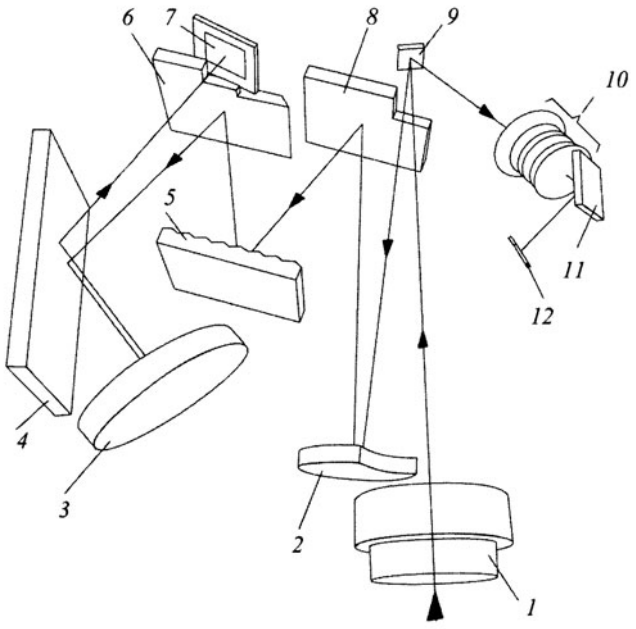

Fig. 1. Optical system for the multi-object spectrometer: 1) projection objective; 2) collimator objective; 3) camera objective; 4, 6, 8) configured mirror (spectroscopic channel); 5) diffraction grating; 7) photodetector (spectroscopic channel); 9) micromirror array; 10) imaging objective (observation channel); 11) configured mirror (observation channel); 12) photodetector (observation channel).

spectral channel are: mismatch between the spectral image of the entrance field and the plane of the detector, and monochromatic aberrations (astigmatism and coma are the most important [17, 18]). Since the latter arise when the light beam passes asymmetrically through the optical system and due to the asymmetry of the optical system itself [18], an obvious way to minimize them is to use optical systems which are as close as possible to axially symmetric, such as the Pfund design [17]. A significant disadvantage of such systems is the aperture losses on cutouts and optical elements used for entrance and exit of the light. We estimate such losses were at least 10% only at the entrance of light to the system for a possible axially symmetric implementation of the polychromator for the multi-object spectrometer. Light losses at the exit would be even higher due to the need to eliminate unacceptable "illumination" of the detector by direct dispersion of light from the diffraction grating: if the detector is "moved away", the sizes of the aperture openings increase even more. This requires a compensating increase in the total numerical aperture of the system and, among other things, leads to an increase in off-axis aberrations at the edge of the field and shading of the least aberrated central portion of the light beam. Increasing the dimensions of the optical elements to decrease the relative significance of the losses is possible only to a fairly small degree, due to limitations on the outside dimensions and a cost that rapidly increases with size. Such effects make it non-optimal to implement the polychromator in the spectral channel as an axially symmetric optical system.

Taking into account the indicated features, we built the polychromator in the spectral channel based on a Czerny–Turner design. A variant of the Ebert–Fastie design is not very suitable in this case due to the large size of the mirror objective and the complexity of choosing the configuration with a large aperture. And the variant of the spherically symmetric Tarasov design [17] gives a characteristic curvature to the image field, which is difficult to correct in the case of a non-point entrance aperture. A characteristic feature of the Czerny design is the presence of off-axis monochromatic aberrations, significantly increasing with a large aperture. In order to reduce the aberrations, the angles of incidence of the light beam on the objectives were minimized, which to some degree can be considered as an approximation of an axially symmetric system but with aperture openings shifted from the centers of the configured

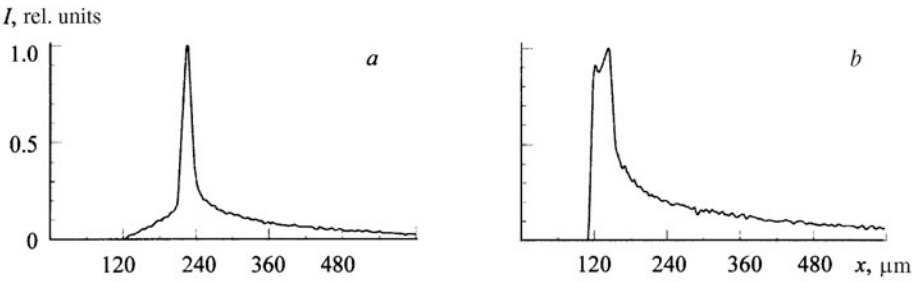

Fig. 2. Typical shape of the cross section of scattering spots in the spectral (a) and spatial (b) directions.

mirrors toward their periphery and transformed to cutouts. As a result, it became possible to bring the configured mirrors closer to the DMD module and the detector in order to reduce the aperture cutouts, the shading was reduced when the light beam entered from outside onto the DMD and from the DMD into the observation channel, and light losses at the peripheral cutouts for most points of the entrance aperture have practically no effect on the low-aberration central portion of the light beam, which has a favorable effect on the overall aberrated image.

Since rotation of a micromirror on switching occurs relative to its diagonal, the light beam reflected from it in the spectral channel or the observation channel lies in a plane perpendicular to the plane of the array and tilted at a 45^{o} angle to its sides. This makes the conventional horizontally symmetric variant of the Czerny–Turner design inapplicable due to the non-optimal formation of a spectral image from the points of the field on the detector. On the other hand, the vertically symmetric variant of the Czerny–Turner design is still inapplicable due to the curvature of the image of the entrance slit present in it, leading to distortions of the spectral image on the detector.

In order to solve this problem, the horizontally symmetric Czerny–Turner design was modified so that the DMD and the detector are removed from the plane of dispersion while the tilt of the collimator objective ensures that the light beam from the DMD enters the plane of dispersion. Such a variant ensures correct scanning of the spectrum on the detector and filling of the optical elements with light, but due to the oblique incidence of the light beam on the objective (in projection onto the plane of dispersion), off-axis aberrations increase somewhat in the system, causing some broadening of the spectral lines.

The tilt of the camera objective ensures that the light flux goes to the detector, shifted in the same half-space relative to the plane of dispersion as the DMD. In contrast to the case of the collimator objective, the light beam passing through the camera objective is axially symmetric in projection onto the plane of dispersion, which makes it possible to reduce off-axis aberrations and to somewhat improve the quality of the spectral image. Due to fact that the light beams pass asymmetrically through the objectives, the coma is asymmetrized (and increases). Nevertheless, this has a better effect on the image quality than symmetrization of the passage of light through the system on the whole, with the aim of reducing coma, since in the presence of an extended entrance field it allows us to more precisely align the focal planes of the spectral images of the DMD pixels with the plane of the detector. From the results shown in Fig. 2 for modeling the scattering spots, we see that coma is present in the system, but due to the asymmetric (in projection onto the plane of dispersion) passage of light only through the collimator objective, aberration broadening of the scattering spot in the direction of scanning the spectrum is less than in the "spatial" direction.

A substantial contribution to degradation of the image quality on the detector comes from the tilt of the plane of the entrance aperture relative to the optic axis of the spectral channel, which is due to features of the DMD. In fact, even in the ideal case of a quasi-planar field for the spectral image of an individual pixel, due to this tilt the image plane of the aperture and a large number of the surfaces for scanning the spectral images of the micromirrors are not aligned (the greater the tilt, the poorer the alignment), which leads to defocusing on the detector. Therefore on the one hand, in order to improve the image quality, the tilt of the entrance aperture relative to the optic axis of the spectral channel should be minimized; on the other hand, due to the fact that the DMD forms two optical channels, such minimization leads to an increase in the analogous angle in the observation channel, which has a negative effect on

image quality in the latter. During modeling, we selected a compromise tilt angle of the DMD relative to the axis of the light beam incident on it, about 6.5°. In this case, in one position of the micromirror, the reflected beam goes into the spectral channel at a 17.5° angle, while in the other position it goes in at a 30.5° angle to the normal of the DMD.

The significant aperture of the hyperspectrometer together with the small angle at which the light beam passes from the DMD to the collimator leads to the latter shading the light beam incident on the DMD, and hence to reduction of the working region of the array. In order to eliminate this, a cutout is called for in the collimator mirror, and the overall aperture of the system is increased to compensate for losses. The photodetector array of the spectral channel is tilted relative to the optic axis, which maintains the symmetry of passage of light in the system as much as possible, allowing us to a significant extent to match the focal planes of the spectral images of the different DMD pixels in the plane of the detector.

The channel is designed only for rough observation of the studied region of space, and so the demands on the quality of the image obtained can be reduced. Nevertheless, a complicating factor in designing its optical system was the need to work with an extended entrance field, tilted at a large angle (~30.5°) relative to the optic axis. Such a tilt makes it unacceptable to use spherical and parabolic mirrors as the imaging objective, since they are sensitive to the depth and extent of the entrance aperture. Therefore we used a refractive objective in the design of the observation channel.

Since when working with a multi-object spectrometer, the width of dynamic scanning of the slit usually is at least two pixels, the size of the detector array in the observation channel can be roughly half the size of the DMD. The linear dimensions of the detector array also were reduced (the DMD image with the decrease), which allowed us, along with using a configured mirror for a "discontinuity" on the optic axis, to reduce the external dimensions of the device.

Basic Optical, Technical, and Analytical Characteristics of the Multi-Object Spectrometer. Design calculations for the elements of the optical system for the multi-object spectrometer were determined mainly by the following requirements: spectral range 400–900 nm, divided into two subranges; spectral resolution ≥0.8 nm; numerical aperture of the spectral channel ≥0.1; and also by the characteristics of the available DMD.

In order to estimate the required size of the detector array in the spectral channel, we can make use of the fact that the usual size of a pixel for modern DMDs is 10–15 μm (12 μm in the model used). Since we need at least three points to specify a spectral line, we can estimate the half-width of a resolved spectral line on the detector: 36 μm. Since this should correspond to at most 0.8 nm of spectrum, the linear dispersion is ~22 nm/mm, while a 270 nm spectral span should fit on ~12 mm of detector. Considering that the dimensions of the DMD are 11 × 8.3 mm, the size of the detector in the direction of the spectral scan should a fortiori be at least 20 mm, and in the direction of the spatial scan it should be at least 11 mm. Considering the fast response requirements, the optimal solution in this case was a Lupa-4000 CMOS array (2048 × 2048 pixels, array size 24.6 × 24.6 mm, pixel size 12 × 12 μm, sampling frequency 66 MHz, signal-to-noise ratio 2000:1).

Numerical modeling showed that the required linear dispersion can be ensured with a grating of 150 lines/mm operating in first order. During modeling, we found the optimal focal length of the objective, 250 mm, ensuring the required linear dispersion (it proved to be equal to 17.2 and 16 nm/mm in the short-wavelength and long-wavelength subranges). Switching between the subranges was done by rotating the diffraction grating by means of a servomechanism commanded by the controlling computer.

Based on the required focal length and the calculated numerical aperture, taking into account compensation of light losses on cutouts (0.12), we selected the diameter of the collimator objective (61 mm) and the camera objective (100 mm). Both have a radius of curvature equal to 500 mm and a focal length of 250 mm. As the imaging objective for the observation channel, we used a Helios-103 photographic objective (f = 53 mm, aperture ratio 1:1.8). Based on the requirements formulated for the camera of the observation channel, we selected a model with a Micron MT9V403 CMOS array (size 6.61 × 4.97 mm, 659 × 494 pixels, pixel size 9.9 × 9.9 μm).

The block diagram for the electronic control system for the multi-object spectrometer is shown in Fig. 3. Our original software made it possible to record the hyperspectrum both from the entire entrance field (hyperspectral mode) and from its fragments (multi-object mode). The operator can specify the width of the micromirror slit, the time and spectral subrange for recording, view and carry out preliminary processing of the data obtained. The most important characteristics of the multi-object spectrometer are given in Table 1.

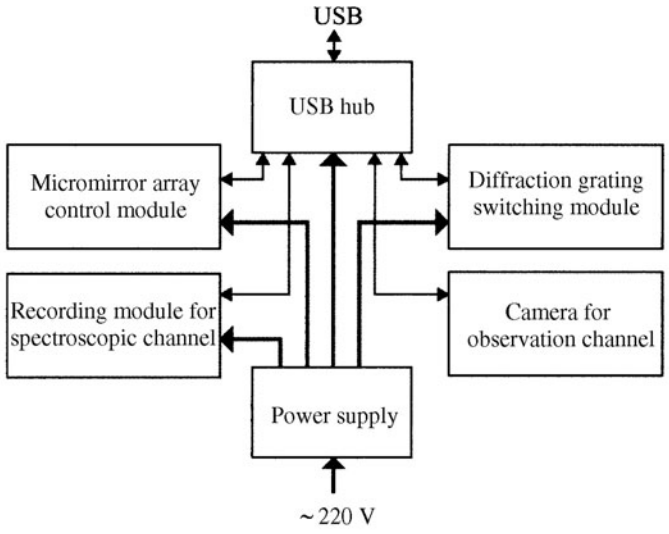

Fig. 3. Block diagram of the electronic control system for the multi-object spectrometer.

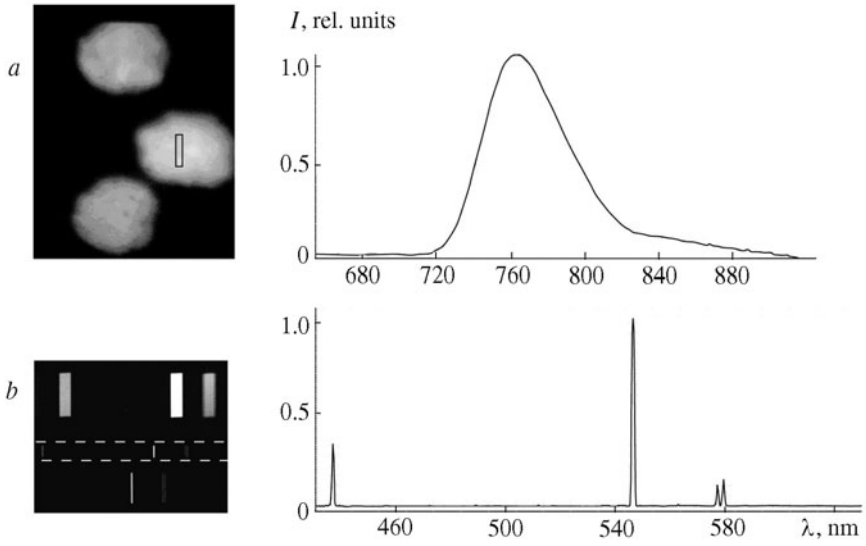

Fig. 4. The shape of the observation channel of the multi-object spectrometer and the spectrum from the isolated region of the section of the paper with the dye (a); fragment of the spectral channel with the corresponding spectrum for illumination of the entrance aperture of the system by a mercury lamp (b).

The measurements showed that the spectral resolution for most of the DMD elements is better than 0.8 nm and only in the most "problematic" sections over the field angles (the fraction of which is no greater than 8% of the total area of the DMD) might it reach 1.1 nm, which on the whole corresponds to the theoretical modeling data (see Table 2).

The capabilities of the multi-object spectrometer are illustrated in Fig. 4. Figure 4a shows the shape of the window for the observation channel of the multi-object spectrometer during test recording of the luminescence of an object, a section of paper with ~0.5 mm spots deposited on it, containing indotricarbocyanine dye (excitation by a semiconductor laser, λ = 685 nm, power 50 mW), and also the spectrum of the region of the dye marked by a rec-

TABLE 1. Basic Analytical Characteristics of the Multi-Object Spectrometer

Characteristic	Value
Spectral resolution,* nm	≤0.8
Spectral working range, nm	395–675, 645–905
Dispersion, nm/mm	17.2 and 16.0
Numerical aperture	0.1 (*f*/5)
Hyperspectrum acquisition time, sec	≤0.3
External dimensions, mm	≤530 × 340 × 280

*For slit width 1 pixel.

TABLE 2. Selected Measurement Results for Testing Spectral Resolution When a Reflective Slit of Width 1 Pixel is Mounted in the Middle of the Micromirror Array

400–670 nm			650–900 nm		
λ, nm	Δλ, nm	$\Delta\lambda_{theor}$, nm	λ, nm	Δλ, nm	$\Delta\lambda_{theor}$, nm
435.8	0.4	0.3	640.2	0.6	0.8
546.1	0.7	0.4	703.3	0.7	0.3
577.0	0.5	0.5	878.0	0.7	0.5

Note. λ is the wavelength of the spectral line, Δλ is the half-width of the line, $\Delta\lambda_{theor}$ is the theoretically calculated half-width of the line.

tangular shape in the observation channel. Figure 4b shows a fragment of the spectral channel for illumination of the entrance aperture of the instrument by a PRK-4 mercury lamp. The isolated rectangular region corresponds to the adjacent spectrum.

Conclusion. We have designed a system for and built a prototype of a multi-object spectrometer for studies in the field of photodynamic therapy. Owing to the use of a new type of spatial light modulator (a micromirror array), we have been able to achieve high spectral and spatial resolution in the hyperspectrum for large aperture within a compact design. The results of an experimental test of the analytical characteristics achieved are evidence that the instrument is suitable for solving a wide range of problems in applied spectroscopy.

REFERENCES

1. M. Borengasser, W. Hungate, and R. Watkins, *Hyperspectral Remote Sensing: Principles and Applications*, CRC, Boca Raton (2007).
2. M. Govender, K. Chetty, and H. Bulcock, *Water S.A.*, **33**, 145–152 (2007).
3. A. Hall, D. Lamb, B. Holzapfel, and J. Louis, *Australian J. Grape and Wine Res.*, **8**, 36–47 (2002).
4. G. Swayze, K. Smith, R. Clark, S. Sutley, R. Pearson, J. Vance, P. Hageman, P. Briggs, A. Meier, M. Singleton, and S. Roth, *Environ. Sci. and Technol.*, **34**, 47–54 (2000).
5. R. Gomez, *Opt. Eng.*, **41**, 2137–2143 (2002).
6. M. Pantazis and D. Thomas, *Proc. SPIE*, **3438**, 31–37 (1998).
7. J. Fisher, M. Baumback, J. Bowles, J. Grossmann, and J. Antoniades, *Proc. SPIE*, **3438**, 23–31 (1998).
8. C. Davis, J. Bowles, R. Leathers, D. Korwan, T. V. Downes, W. Snyder, W. J. Rhea, W. Chen, J. Fisher, W. P. Bissett, and R. Reisse, *Opt. Express*, **10**, 210–221 (2002).
9. M. Schaepman and K. Itten, *Proc. SPIE*, **5234**, 202–210 (2003).
10. T. Weser, F. Rottensteiner, J. Willneff, and C. Fraser, *The International Archives of the Photogrammetry, Remote Sensing and Spatial Information Sciences, Pt. B1, Beijing*, **37**, 723–729 (2008).

11. R. Green, M. Eastwood, C. Sarture, T. Chrien, M. Aronsson, B. Chippendale, J. Faust, B. Pavri, C. Chovit, M. Solis, M. Olah, and O. Williams, *Remote Sens. Environ*., **65**, 227–248 (1998).
12. M. Sinclair, J. Timlin, D. Haaland, and M. Werner-Washburne, *Appl. Opt*., **43**, 2079–2088 (2004).
13. V. Pustovoit and V. Pozhar, *J. Acoust. Soc. Am*., **123**, 3143 (2008).
14. A. Harvey and D. Fletcher-Holmes, *Opt. Express*, **12**, 5368–5374 (2004).
15. A. Barducci, P. Marcoionni, and I. Pippi, *Ann. Geophys*., **49**, 103–107 (2006).
16. R. Meyer, K. Kearney, Z. Ninkov, C. Cotton, P. Hammond, and B. Statt, *Proc. SPIE*, **5492**, 200–219 (2004).
17. V. A. Vagin, M. A. Gershun, G. N. Zhizhin, and K. I. Tarasov, *Wide-Aperture Spectral Instruments* [in Russian], Nauka, Moscow (1988).
18. K. I. Tarasov, *Spectral Instruments* [in Russian], Mashinostroenie, Leningrad (1977)